Published in final edited form as:
Cancer Res. 2012 February 1; 72(3): 604–615. doi:10.1158/0008-5472.CAN-11-0669.

S100A7 enhances mammary tumorigenesis through upregulation of inflammatory pathways

Mohd W. Nasser[1], **Zahida Qamri**[1], **Yadwinder S. Deol**[1], **Janani Ravi**[1], **Catherine A. Powell**[1], **Prashant Trikha**[2], **Reto A. Schwendener**[3], **Xue-Feng Bai**[1], **Konstantin Shilo**[1], **Xianghong Zou**[1], **Gustavo Leone**[2], **Ronald Wolf**[4], **Stuart H. Yuspa**[5], and **Ramesh K. Ganju**[1]

[1]Department of Pathology, The Ohio State University, Columbus, Ohio [2]Molecular Cancer Genetics, The Ohio State University, Columbus, Ohio [3]Institute of Molecular Cancer Research, University of Zurich, Zurich, Switzerland [4]Department of Dermatology and Allergology, Ludwig Maximilian University, Munich, Germany. [5]Laboratory of Cancer Biology and Genetics, National Cancer Institute, Bethesda, Maryland 20892, USA.

Abstract

S100A7/Psoriasin, a member of the epidermal differentiation complex, is widely overexpressed in invasive ER-negative (ERα-) breast cancers. However, it has not been established whether S100A7 contributes to breast cancer growth or metastasis. Here, we report the consequences of its expression on inflammatory pathways that impact breast cancer growth. Overexpression of human S100A7 or its murine homolog mS100a7a15, enhanced cell proliferation and upregulated various pro-inflammatory molecules in ERα- breast cancer cells. To examine *in vivo* effects, we generated mice with an inducible form of mS100a7a15 (MMTV-mS100a7a15 mice). Orthotopic implantation of MVT-1 breast tumor cells into the mammary glands of these mice enhanced tumor growth and metastasis. Compared to uninduced transgenic control mice, the mammary glands of mice where mS100a7a15 was induced exhibited increased ductal hyperplasia and expression of molecules involved in proliferation, signaling, tissue remodeling and macrophage recruitment. Furthermore, tumors and lung tissues obtained from these mice showed further increases in pro-metastatic gene expression and recruitment of tumor-associated macrophages (TAMs). Notably, in vivo depletion of TAM inhibited the effects of mS100a7a15 induction on tumor growth and angiogenesis. Further, introduction of soluble hS100A7 or mS100a7a15 enhanced chemotaxis of macrophages via activation of RAGE receptors. In summary, our work employed a powerful new model system to demonstrate that S100A7 enhances breast tumor growth and metastasis by activating proinflammatory and metastatic pathways.

Introduction

The human S100A7 (hS100A7) gene is present within the epidermal differentiation complex on 1q21 chromosome (1) and is predominantly expressed in high-grade ductal carcinoma *in situ* (DCIS) (2-6). In addition, its expression is significantly associated with ERα- and nodal metastasis in invasive ductal tumors (2, 4-6). Furthermore, hS100A7 expression is associated with increased angiogenesis (7). hS100A7 has been shown to modulate tumor growth by activating several signaling pathways (5, 8-10).

Address for correspondence: Ramesh K. Ganju, Department of Pathology, Ohio State University, 185 Hamilton Hall, 1645 Neil Ave, Columbus, OH 43210, Tel: 614-292-5539; Fax: 614-292-7072; Ramesh.Ganju@osumc.edu.

The authors declare that they have no potential conflicts of interest.

hS100A7 has also been associated with increased inflammatory cell infiltrates in invasive breast tumors (2) and various inflammatory disorders (2). Cytokines, including OSM, IL-6 and IL-1, have been shown to induce hS100A7 (10). These cytokines directly or indirectly signal through STAT3 pathways (11, 12). STAT3 has been shown to be constitutively activated in 35%-60% of human breast cancers (13). Activated STAT3 has also been shown to be associated with increased expression of cytokines, growth factors, matrix-metalloproteinases (MMPs) and angiogenic factors (12). In addition, STAT3 signaling modulates tumor growth and metastasis by recruitment of TAMs to tumors (14, 15). TAMs, which often constitute a major part of leukocyte infiltrates present in the tumor microenvironment, have been shown to enhance the tumor growth and metastasis of various cancers (16, 17). In addition, collaborative interactions of tumors with TAMs have been associated with poor prognosis in breast cancer (16, 18). Studies with mouse models have demonstrated that ablation of macrophages leads to inhibition of tumor progression and metastasis (19-21). Factors produced by tumor cells, especially cytokines/chemokines, activate TAMs, which in turn release factors that stimulate tumor cell proliferation, angiogenesis and metastasis (17, 20).

Transgenic mouse models of human breast cancer have provided important information regarding the initiation and progression of breast cancer and thus have emerged as powerful tools for preclinical research. Phylogenetic analyses have shown the mouse ancestor mS100a7a15 to be most related to S100A7 and S100A15 among the human paralogs (22, 23). mS100a7a15 has been shown to be upregulated in carcinogen-induced mammary tumorigenesis (22). However, the direct functional role of mS100a7a15 in disease progression is not well-characterized. In the present investigation, we have generated a novel transgenic mouse model MMTV-rtTA; tetO-mS100a7a15 (MMTV-mS100a7a15) to study the functional significance of mS100a7a15 in breast tumorigenesis. We have used this model to analyze the role of mS100a7a15 in breast cancer growth/metastasis and have shown that mS100a7a15 may enhance tumorigenesis by inducing pro-inflammatory molecules and recruiting TAMs.

Materials and Methods

Cell culture and transfection

Human breast carcinoma cell line MDA-MB-231 (ATCC) and MVT-1 cells derived from MMTV-c-Myc; MMTV-VEGF bi-transgenic mice (obtained from Dr. Johnson) were cultured (24, 25). The identity of these cell lines was regularly verified on the basis of cell morphology. cDNA of hS100A7 (OriGene Technologies) and cDNA of mS100a7a15 were subcloned into pIRES2-EGFP (Invitrogen). Cells were transfected with pIRES2-EGFP-hS100A7 or pIRES2-EGFP-mS100a7a15 or pIRES-2-EGFP using Lipofectamine reagent according to the manufacturer's instructions and stable clones were generated using G418 (500 μg/ml).

Cell Proliferation

Cell proliferation of hS100A7 and mS100a7a15 overexpressing MDA-MB-231 was determined as described (24).

Chemotaxis

The chemotactic assays were performed using transwell chambers (Costar 8 μm pore size) (24). Briefly, phorbol myristic acid (PMA 100 ng/ml)-THP1-differentiated macrophages (TDM) or murine macrophage RAW264.7 cells (MMR) were serum starved. Top chambers were loaded with 150μl of 1×10^6 cells/ml in serum-free medium (SFM) and bottom chambers had 600 μl of SFM containing 50 μg of concentrated supernatant obtained from

hS100A7- or mS100a7a15-overexpressing or vector-expressing MDA-MB-231 cells. Migrated cells were fixed and documented as described (24).

Western Blot Analysis

Western blot (WB) analysis of lysates was done as described (24).

Microarray analysis

Total RNA was collected from hS100A7-overexpressing MDA-MB-231 cells or Vec using TRIzol reagent (Invitrogen). Microarray analysis was done at the Ohio State University (OSU) core facility using an Affymetrix Microarray gene U133 chip containing 40,000 human genes. The data was deposited in the GEO Expression Omnibus under accession no. GSE32052 (Table S-1).

Generation of transgenic mice

TetO-mS100a7a15 mice (26) were cross-bred with MMTV-rtTA (provided by Dr. Chodosh) mice to generate bi-transgenic MMTV-mS100a7a15 mice. Transgenic littermates were genotyped by PCR using tetO-mS100a7a15 primers (Table S-1). Female mice were fed with Dox-chow 1g/kg (Harlan laboratories) and mice fed with normal diet served as controls. All transgenic mice were kept in OSU's animal facility in compliance with the guidelines and protocols approved by the IACUC.

Wholemount analysis of mammary glands

Right inguinal mammary gland (MG) #4 were spread on glass slides, fixed and stained overnight with 0.2% (w/v) carmine (Sigma) and 0.5% (w/v) aluminum sulfate (Sigma) as described (27).

Orthotopic injection assay

1×10^5 /100 μl of murine MVT-1 cells were injected into MG (#4) of transgenic mice. Injected mice were either fed with Dox-chow 1g/kg for 28 days or normal diet (control). Tumors were measured weekly with external calipers and volume was calculated according to the formula $V = 0.52 \times a^2 \times b$, where a is the smallest superficial diameter and b is the largest superficial diameter. Orthotopically injected animals were sacrificed 28 days post-injection and tumors were excised and processed (28).

Depletion of macrophages using clodronate liposomes

Clodronate liposomes (Clodrolip) were prepared as described (21). Briefly, Clodrolip (1.5 mg/kg) was injected intraperitoneally (i.p.) 6 h after tumor cell implantation and followed by 0.75 mg/kg treatments every 4 days. Control groups received PBS-liposomes at the same time points. The mice were sacrificed 25 days post-injection and tumors were excised and processed.

FACS Analysis

For FACS analysis, freshly prepared single cell suspension of tumor-infiltrating cells were incubated with anti-F4/80 PE, anti-Cd11b APC and anti-CD206 Alexa Flour 488 (29). Receptor for advanced glycation end products (RAGE) expression was analyzed by staining with RAGE antibody (Abcam) followed by Alexa Flour 488 antibody. After staining, the cells were analyzed by FACS Caliber using CellQuest software (BD Biosciences).

Immunohistochemistry (IHC)

Samples from MG and tumors were dissected, fixed in formalin and embedded in paraffin for sections. Standard IHC techniques were used according to the manufacturer's recommendations (Vector Laboratories) using antibodies against Ki67 (Neomarkers, 1:100), CD31 (Santa Cruz 1:100), Keratin-8 (Troma-1 1:100), mS100a7a15 (custom, 1:250), F4/80 (AbD Serotec, 1:50), arginase1 (Santa Cruz, 1:200), and rabbit anti-mouse iNOS (Abcam, 1:200) for 60 min at room temperature. Vectastain Elite ABC reagents (Vector Laboratories), using avidin DH:biotinylated horseradish peroxidase H complex with 3,3′-diaminobenzidine (Polysciences) and Mayer's hematoxylin (Fisher Scientific), were used for detection of the bound antibodies.

Reverse Transcriptase and Real-time PCR

RNA was isolated from cells, mouse MG and tissues using TRIzol reagent (Invitrogen). Reverse transcriptase PCR (RT-PCR) reaction was done using RT-PCR kits (Applied Biosystem, CA). Expression of genes analyzed by q-PCR was normalized to GAPDH using the $2^{-\Delta CT}$ method (30). Primers used for RT-PCR and q-PCR are listed in table S-1.

Statistical Analysis

Student's t test was used to compare different experimental groups. $P < 0.05$ was considered to be statistically significant. For all graphs, * indicates $P < 0.05$; ** indicates $P < 0.01$.

Results

hS100A7 and mS100a7a15 overexpression induces proliferation and expression of inflammatory cytokines/chemokines

hS100A7 has been shown to be highly associated with ERα$^-$ breast cancers. Therefore, we first analyzed the effect of hS100A7 overexpression on proliferation of the ERα$^-$ MDA-MB-231 cell line using two different clones, S1 and S2. hS100A7 expression was confirmed by Western blot (WB) (Fig. 1*A*, *left*). hS100A7 overexpression significantly enhanced growth in both the clones, compared to vector control (Vec) (Fig. 1A *right*). To determine the mechanism by which hS100A7 may enhance tumorigenesis, we carried out microarray analysis and found that hS100A7 overexpression induced high levels of pro-inflammatory cytokines/chemokines CXCL1, CXCL8, IL-1α, IL-11 and CSF2 as compared to control (Fig. 1B). The expression of these hS100A7-induced target proteins was further confirmed using q-PCR in two different clones, S1 and S2 (Fig. 1C).

Phylogenetic analyses have shown that mS100a7a15 is most related to hS100A7 and hS100A15 (22, 23). mS100a7a15 has also been shown to be associated with inflammation (31). Similar to hS100A7, mS100a7a15 overexpression in two different clones of MDA-MB-231 (M1 and M2) enhanced proliferation (Fig. 1D *lower*) and expression of inflammatory molecules CXCL1, CXCL8, IL-1α, IL-11 and CSF2 as compared to Vec (Fig. 1E). These results suggest that hS100A7 and mS100a7a15 overexpression enhance growth and upregulate pro-inflammatory cytokine/chemokine production in breast cancer cells.

mS100a7a15 induces mammary hyperplasia in bi-transgenic mice

It has been reported that mS100a7a15 is up-regulated during carcinogen-induced mammary tumorigenesis (22). However, to the best of our knowledge, there is no transgenic/knockout mouse model available to study the role of mS100a7a15 in breast tumorigenesis. Very recently K5-tTA; tetO-mS100a7a15 mice were generated for studying the role of mS100a7a15 in psoriasis (26). To determine the role of mS100a7a15 in tumorigenesis, we generated an inducible-transgenic mouse model by crossing tetO-mS100a7a15 mice with

tetracycline-responsive transactivator protein under the murine mammary tumor virus (MMTV-rtTA) promoter mice. In the presence of doxycycline, rtTA protein changes its conformation and binds to *tet* operator (tet-O) sequences that result in expression of mS100a7a15 in mammary epithelial cells (Fig. 2A). The mice were genotyped with mS100a7a15 and MMTV-rtTA specific primers (data not shown). MG derived from MMTV-mS100a7a15 mice that were subjected to Dox-chow (1g/kg) for three months showed mS100a7a15 expression at mRNA levels (Fig. 2B, *right*). We also observed enhanced mS100a7a15 expression in these mice by IHC (Fig. 2B, *left*). We further identified the mS100a7a15-overexpressing cells to be of luminal epithelial origin as these cells also express CK8 (Fig. 2B, *left*). Further morphological examination of whole-mount virgin MG by carmine (Fig. 2C *upper*) or hematoxylin and eosin (H&E) (Fig. 2C, *lower*) staining demonstrated ductal hyperplasia in the Dox-induced MMTV-mS100a7a15 mice compared to uninduced mice. These findings indicate that overexpression of mS100a7a15 in mouse MG induces hyperplasia.

mS100a7a15 overexpression in mammary glands enhances proliferative, inflammatory, and signaling pathways

We analyzed the expression of phospho-STAT3, phospho-AKT, phospho-ERK and cyclinD1 in MG as these molecules have been shown to be associated with pro-inflammatory and proliferative responses and are activated in breast cancer tissue (12, 13, 32). We observed enhanced phosphorylation of STAT3, ERK and AKT in Dox-treated MMTV-mS100a7a15 mice (Fig. 2D). We also observed enhanced expression of cyclin D1 by WB (Fig. 2D) and expression of Ki67 and cyclinD1 by IHC (Fig. 2E) in Dox-induced MMTV-mS100a7a15 mice. Since STAT3 has been shown to enhance macrophage infiltrations to the tumors (12), we further analyzed the recruitment of macrophages in the MG of these mice. We found an increase in macrophages in Dox-induced MMTV-mS100a7a15 compared to uninduced mice (Fig. 2E). MMPs are known to degrade ECM proteins in the cellular microenvironment and significant correlation between TAM count and MMP expression has been observed in tumor (33-35). We observed enhanced MMP2 expression in the MG of Dox-induced MMTV-mS100a7a15 compared to uninduced mice (Fig. 2D). These data indicate that mS100a7a15 overexpression induces hyperplasia, activates STAT3/AKT/ERK pathways and enhances the macrophage recruitment.

mS100a7a15 enhances tumor growth in an orthotopic syngeneic breast cancer model

hS100A7 has been shown to increase tumor growth in nude mice (5, 7). We further analyzed the role of mS100a7a15 in tumor progression, by implanting highly aggressive MVT-1 cells (25) into the MG of MMTV-mS100a7a15 mice. Five days prior to injection, mice (n=5) were fed with 1g/kg Dox-chow to induce mS100a7a15 and mice maintained on normal diet served as control. These mice were observed for tumor growth (Fig. 3A *left*). Interestingly, MVT-1-derived tumor growth was enhanced two-fold in Dox-treated MMTV-mS100a7a15 compared to the uninduced mice (Fig. 3A, *middle* and *right*). These studies demonstrate that mS100a7a15 expression in MG enhanced growth of breast cancer cells in syngeneic mouse models.

mS100a7a15 overexpression enhances TAM recruitment in a syngeneic mouse model

TAMs have been shown to be a major component of inflammatory infiltrates seen in tumors (18, 20). Initially, MVT-1 derived primary tumors were evaluated by IHC with macrophage marker F4/80. $F4/80^+$ macrophages were enhanced in tumor tissues of Dox-induced MMTV-mS100a7a15 compared to uninduced mice (Fig. 3B). We further analyzed macrophage infiltration in the tumors by flow cytometry. As shown in Fig. 3C, the $CD11b^+/F4/80^+$ macrophage infiltration was increased by ~42% in Dox-induced MMTV-mS100a7a15 compared to uninduced mice. We also analyzed other cell types such as Gr-1,

T- and B cells, but did not notice any significant increase in the Dox-induced MMTV-mS100a7a15 compared to uninduced mice (data not shown).

TAMs can be divided into two main classes, tumor-suppressive M1 (classically activated) and tumor-promoting M2 (alternative). M1 macrophages are characterized among other factors by expression of inducible nitric oxide synthase (iNOS) while M2 macrophages have a decreased level of iNOS and are identified by their signature expression of arginase-1 (Arg-1) and mannose receptor (CD206) (36). An increase of 29% $CD11b^+/CD206$ (M2 TAM) was observed in tumors derived from Dox-induced MMTV-mS100a7a15 compared to uninduced mice (Fig. 3D). We further confirmed increased M2 phenotype by IHC for enhanced expression of Arg-1 and decreased iNOS expression (Fig. 3E *left*). Changes in expression of Arg-1 or iNOS were also detected by q-PCR (Fig. 3E *right*). These results suggest that mS100a7a15 may enhance tumor growth by recruiting M2 macrophages to the tumor site.

mS100a7a15 overexpression induces the expression of metastatic and angiogenic markers

We examined the expression of pro-metastatic and angiogenic genes such as CCL2, Cox2, MMP9 and VEGF in the MVT-1 derived tumors. These genes were significantly upregulated in Dox-induced MMTV-mS100a7a15 compared to uninduced mice (Fig. 4A and B). We also observed a ~2.7 fold increase in $CD31^+$ blood vessels as detected by IHC in Dox-induced MMTV-mS100a7a15 compared to uninduced mice (Fig. 4C and D). These studies suggest that mS100a7a15 may enhance expression of metastatic and angiogenic markers.

mS100a7a15 overexpression enhances metastasis in orthotopic breast cancer models

We further investigated the role of mS100a7a15 on spontaneous metastasis in MMTV-mS100a7a15 mice injected with MVT-1 cells. We observed a significant increase in surface lung metastases in the mice treated with Dox compared to untreated mice ($p<0.049$) (Fig. 5A and B). Since TAMs have been shown to enhance metastasis (17, 18, 20), we further analyzed the infiltrations of macrophages in the lung tissues and observed enhanced expression of F4/80+ macrophages (Fig. 5C) and Arg-1 expression but decreased iNOS expression (Fig. 5C) in Dox-induced MMTV-mS100a7a15 compared to untreated mice. We also observed a significant increase in pro-metastatic genes, such as CCL2 and VEGF, in the metastatic lung tissue of Dox-induced MMTV-mS100a7a15 compared to uninduced mice (Fig. 5D). These studies suggest that mS100a7a15 may enhance metastasis through enhancement of pro-metastatic genes in the metastatic lungs.

Macrophage depletion inhibits tumor growth and angiogenesis

To specifically analyze the role of mS100a7a15 overexpression in TAMs recruitment, we selectively inhibited macrophages using clodrolip (liposome encapsulated clodronate) as previously described (21). Clodrolip treatment significantly reduced tumor growth in MVT-1-derived Dox-induced MMTV-mS100a7a15 compared to control-liposome treated mice (Fig. 6A and B). Quantification of the number of $F4/80^+$ TAMs and $CD206^+$ M2 TAMs by FACS (Fig 6C) and IHC (Fig. 6D and E *left*) revealed a significant decrease in TAMs and M2 TAMs in clodrolip treated compared to control-liposome treated mice fed with Dox diet (Fig. 6D and E). We also observed significant reduction in angiogenesis as detected by $CD31^+$ IHC staining in clodrolip treated MMTV-mS100a7a15 compared to control-liposome treated mice fed with Dox diet (Fig. 6 *D lower and 6E right)*. These studies further confirm that mS100a7a15 may enhance tumorigenesis and angiogenesis through recruitment of macrophages.

Soluble hS100A7 and mS100a7a15 enhances chemotaxis in macrophages *in vitro*

Previously, soluble hS100A7 and mS100a7a15 were shown to induce chemotaxis in leukocytes by binding to RAGE (26, 37). However, not much is known about the role of these proteins in regulating monocyte/macrophage chemotaxis. We analyzed the effect of hS100A7 secreted into the conditioned media (CM) on chemotaxis of the differentiated monocytic cell line THP-1. hS100A7 expression was observed in the supernatant of hS100A7-overexpressing MDA-MB-231 cells (Fig. 7*A*, *left*). We also observed expression of RAGE in TDM (Fig. 7*A*, *right*). Furthermore, we observed a significant increase in the chemotaxis of TDM upon stimulation with CM of hS100A7-MDA-MB-231 cells. These effects were significantly abrogated by blocking RAGE (Fig. 7*B*). We have also shown that RAGE is expressed on the surface of MMR (Fig. 7C). We also observed mS100a7a15 expression in the CM of mS100a7a15-overexpressing MDA-MB-231 cells (Fig. 7C, *right*). In addition, CM of mS100a7a15-expressing MDA-MB-231 cells enhanced migration of MMR and these effects were blocked by murine RAGE neutralizing antibodies (Fig. 7D). These studies suggest that hS100A7/mS100a7a15 may enhance monocyte/macrophage chemotaxis through RAGE.

Discussion

hS100A7 has been shown to be associated with the ERα$^-$ phenotype and is predominantly expressed in high-grade DCIS. Furthermore, expression of hS100A7 in breast tumors represents a poor prognostic marker and correlates with lymphocyte infiltration and high-grade morphology (2, 6, 7). Although a number of putative functions have been proposed for hS100A7, its biological role particularly in breast cancer remains to be defined.

In the present study, we characterized the tumor enhancing effects of hS100A7 and mS100a7a15 in MDA-MB-231 breast cancer cells and inducible MMTV-mS100a7a15 mouse model systems. We observed enhanced proliferation and production of pro-inflammatory molecules IL-1α, IL-11, CSF2, CXCL1 and CXCL8 in hS100A7 and mS100a7a15-overexpressing cells compared to vector control. These molecules have been shown to play a major role in tumor progression and invasion (38, 39).

In an inducible transgenic mouse model system, we observed a significant increase in the number of primary ducts and side branches in mice expressing mS100a7a15 in mammary epithelial cells. This increase in mammary ductal epithelial hyperplasia was caused by enhanced proliferation as indicated by increased expression of Ki67 and cyclin D1 in the ductal epithelial cells of induced mice. We observed increased expression of STAT3 and MMP-2 in MG of inducible mice. Overexpression of cyclin D1 has been reported in up to 50% of primary breast tumors (40). In addition, STAT3 has been shown to be constitutively activated in 35 to 60% of breast cancers (12).

We also showed that mS100a7a15 overexpression significantly increased tumor growth in the syngeneic orthotopic model. Further elucidation of mechanisms revealed that mS100a7a15 may enhance growth and metastasis through recruitment of M2 TAMs. M2 polarized TAMs are known to drive tumor progression by stimulating angiogenesis and metastasis (17, 18, 20). We have shown that M2 specific markers are increased while expression of M1 markers is decreased in MVT-1-derived tumors and lung tissues of Dox-induced mS100a7a15 mice. We further determined whether selective depletion of macrophages would inhibit tumor growth. It has been shown previously that macrophages may be selectively depleted in mice using clodrolip (21). Therefore, we treated MVT-1 tumor bearing mice with intraperitoneal inoculations of clodrolip or with an empty liposome control at various points throughout tumor progression. We observed ~80% depletion of macrophage content of the tumors compared to control-liposome treated tumors in Dox-

induced MMTV-S100a7a15 mice. We also observed that clodrolip-mediated reduction of TAMs also caused dramatic reduction in tumor growth in Dox-induced MMTV-mS100a7a15 mice. These results suggest that mS100a7a15 may enhance tumor growth through enhancing recruitment of macrophages to the tumors. Previous studies have reported that an intimate relationship between macrophages and tumor cells is required for tumor growth and metastasis (18, 41). We have shown hS100A7 and mS100a7a15 enhanced chemotaxis of monocyte/macrophages through RAGE. RAGE expression has been detected in a variety of human tumors including breast (42). It has been shown that the blockade of RAGE in glioma suppressed tumor growth (43).

Although mS100a7a15 has been shown to enhance CD4-positive T-cell populations in mS100a7a15 overexpressing keratinocytes from psoriasis mouse model (26), we did not observe a significant change in CD4-positive T-cells as detected by FACS in tumors derived from our MVT-1 orthotopic syngeneic model. This difference may be attributed to the different model systems used in each study. Another possibility is that the recruitment of macrophages could result from enhanced production of chemokine CCL2 in tumors from Dox-induced MMTV-mS100a7a15 mice. CCL2 has been shown to recruit inflammatory monocytes/macrophages that in turn stimulate breast tumor growth and metastasis (44). In breast cancer, macrophage infiltration and CCL2 expression have been correlated with metastatic disease and poor prognosis (45-47).

We also observed significant increase in spontaneous metastasis and M2 TAMs in orthotopic syngeneic MMTV-mS100a7a15 mouse model. Previous studies have shown that TAMs promote metastasis by enhancing pro-metastatic and proangiogenic activities within the tumor microenvironment (17, 18, 20). We have shown enhanced expression of pro-metastatic and pro-angiogenic molecules such as CCL2 and VEGF in metastatic lung tissues. Also, we observed enhanced expression of CCL2, VEGF, Cox2, and MMP9 in primary tumors. These molecules have been shown to enhance metastasis of various cancers (33, 44, 48-50). Previously, it has been shown that hS100A7 modulates VEGF expression in MDA-MB-468 cells (7). These studies suggest hS100A7 which has been shown to be associated with highly-invasive breast cancer subtypes (31) may enhance metastasis through enhancement of pro-metastatic and angiogenic molecules.

In summary, using a novel mS100a7a15 transgenic and orthotopic syngeneic mouse models, we have shown that mS100a7a15 overexpression in mammary epithelial cells enhances hyperplasia, tumor growth, angiogenesis and metastasis. As shown in model (Fig. S-1), our studies for the first time revealed that hS100A7/mS100a7a15 produced by epithelial cells may enhance proliferation and recruit TAMs to tumor site by endocrine mechanism through RAGE activation. Recruitment of TAMs into tumor microenvironment may in turn stimulate tumor growth and metastasis by enhancing expression of pro-metastatic and pro-inflammatory molecules such as CCL2, Cox2, MMP9 and VEGF. Thus, these studies suggest that S100A7 may enhance tumor growth and metastasis especially in $ER\alpha^-$ tumors, through a novel mechanism by activating proinflammatory and metastatic pathways.

Supplementary Material

Refer to Web version on PubMed Central for supplementary material.

Acknowledgments

We thank Susie Jones for IHC, Mohamed Adel, and Zameer Gill for technical help. YSD was supported by Pelotonia Fellowship from the Comprehensive Cancer Center, OSU. This work was supported in part by grants from National Institutes of Health (CA109527 and CA153490) and Department of Defense to RKG.

Abbreviations

S100A7	Psoriasin
TAM	tumor associated macrophage
Stat3	Signal transducer and activator of transcription 3

References

1. Donato R. S100: a multigenic family of calcium-modulated proteins of the EF-hand type with intracellular and extracellular functional roles. Int J Biochem Cell Biol. 2001; 33:637–68. [PubMed: 11390274]
2. Al-Haddad S, Zhang Z, Leygue E, Snell L, Huang A, Niu Y, et al. Psoriasin (S100A7) expression and invasive breast cancer. Am J Pathol. 1999; 155:2057–66. [PubMed: 10595935]
3. Enerback C, Porter DA, Seth P, Sgroi D, Gaudet J, Weremowicz S, et al. Psoriasin expression in mammary epithelial cells in vitro and in vivo. Cancer Res. 2002; 62:43–7. [PubMed: 11782356]
4. Emberley ED, Murphy LC, Watson PH. S100A7 and the progression of breast cancer. Breast Cancer Res. 2004; 6:153–9. [PubMed: 15217486]
5. Emberley ED, Niu Y, Leygue E, Tomes L, Gietz RD, Murphy LC, et al. Psoriasin interacts with Jab1 and influences breast cancer progression. Cancer Res. 2003; 63:1954–61. [PubMed: 12702588]
6. Emberley ED, Niu Y, Njue C, Kliewer EV, Murphy LC, Watson PH. Psoriasin (S100A7) expression is associated with poor outcome in estrogen receptor-negative invasive breast cancer. Clin Cancer Res. 2003; 9:2627–31. [PubMed: 12855640]
7. Krop I, Marz A, Carlsson H, Li X, Bloushtain-Qimron N, Hu M, et al. A putative role for psoriasin in breast tumor progression. Cancer Res. 2005; 65:11326–34. [PubMed: 16357139]
8. Emberley ED, Niu Y, Curtis L, Troup S, Mandal SK, Myers JN, et al. The S100A7-c-Jun activation domain binding protein 1 pathway enhances prosurvival pathways in breast cancer. Cancer Res. 2005; 65:5696–702. [PubMed: 15994944]
9. Paruchuri V, Prasad A, McHugh K, Bhat HK, Polyak K, Ganju RK. S100A7-downregulation inhibits epidermal growth factor-induced signaling in breast cancer cells and blocks osteoclast formation. PLoS ONE. 2008; 3:e1741. [PubMed: 18320059]
10. West NR, Watson PH. S100A7 (psoriasin) is induced by the proinflammatory cytokines oncostatin-M and interleukin-6 in human breast cancer. Oncogene. 2010; 29:2083–92. [PubMed: 20101226]
11. Perrier S, Caldefie-Chezet F, Vasson MP. IL-1 family in breast cancer: potential interplay with leptin and other adipocytokines. FEBS Lett. 2009; 583:259–65. [PubMed: 19111549]
12. Ranger JJ, Levy DE, Shahalizadeh S, Hallett M, Muller WJ. Identification of a Stat3-dependent transcription regulatory network involved in metastatic progression. Cancer Res. 2009; 69:6823–30. [PubMed: 19690134]
13. Hsieh FC, Cheng G, Lin J. Evaluation of potential Stat3-regulated genes in human breast cancer. Biochem Biophys Res Commun. 2005; 335:292–9. [PubMed: 16081048]
14. Clarkson RW, Boland MP, Kritikou EA, Lee JM, Freeman TC, Tiffen PG, et al. The genes induced by signal transducer and activators of transcription (STAT)3 and STAT5 in mammary epithelial cells define the roles of these STATs in mammary development. Mol Endocrinol. 2006; 20:675–85. [PubMed: 16293640]
15. Niu G, Wright KL, Huang M, Song L, Haura E, Turkson J, et al. Constitutive Stat3 activity up-regulates VEGF expression and tumor angiogenesis. Oncogene. 2002; 21:2000–8. [PubMed: 11960372]
16. Allavena P, Sica A, Solinas G, Porta C, Mantovani A. The inflammatory micro-environment in tumor progression: the role of tumor-associated macrophages. Crit Rev Oncol Hematol. 2008; 66:1–9. [PubMed: 17913510]
17. Sica A, Allavena P, Mantovani A. Cancer related inflammation: the macrophage connection. Cancer Lett. 2008; 267:204–15. [PubMed: 18448242]

18. Pollard JW. Tumour-educated macrophages promote tumour progression and metastasis. Nat Rev Cancer. 2004; 4:71–8. [PubMed: 14708027]
19. Lin EY, Nguyen AV, Russell RG, Pollard JW. Colony-stimulating factor 1 promotes progression of mammary tumors to malignancy. J Exp Med. 2001; 193:727–40. [PubMed: 11257139]
20. Lin EY, Pollard JW. Tumor-associated macrophages press the angiogenic switch in breast cancer. Cancer Res. 2007; 67:5064–6. [PubMed: 17545580]
21. Zeisberger SM, Odermatt B, Marty C, Zehnder-Fjallman AH, Ballmer-Hofer K, Schwendener RA. Clodronate-liposome-mediated depletion of tumour-associated macrophages: a new and highly effective antiangiogenic therapy approach. Br J Cancer. 2006; 95:272–81. [PubMed: 16832418]
22. Webb M, Emberley ED, Lizardo M, Alowami S, Qing G, Alfia'ar A, et al. Expression analysis of the mouse S100A7/psoriasin gene in skin inflammation and mammary tumorigenesis. BMC Cancer. 2005; 5:17. [PubMed: 15717926]
23. Wolf R, Voscopoulos CJ, FitzGerald PC, Goldsmith P, Cataisson C, Gunsior M, et al. The mouse S100A15 ortholog parallels genomic organization, structure, gene expression, and protein-processing pattern of the human S100A7/A15 subfamily during epidermal maturation. J Invest Dermatol. 2006; 126:1600–8. [PubMed: 16528363]
24. Qamri Z, Preet A, Nasser MW, Bass CE, Leone G, Barsky SH, et al. Synthetic cannabinoid receptor agonists inhibit tumor growth and metastasis of breast cancer. Mol Cancer Ther. 2009; 8:3117–29. [PubMed: 19887554]
25. Pei XF, Noble MS, Davoli MA, Rosfjord E, Tilli MT, Furth PA, et al. Explant-cell culture of primary mammary tumors from MMTV-c-Myc transgenic mice. In Vitro Cell Dev Biol Anim. 2004; 40:14–21. [PubMed: 15180438]
26. Wolf R, Mascia F, Dharamsi A, Howard OM, Cataisson C, Bliskovski V, et al. Gene from a psoriasis susceptibility locus primes the skin for inflammation. Sci Transl Med. 2010; 2:61ra90.
27. Trimboli AJ, Cantemir-Stone CZ, Li F, Wallace JA, Merchant A, Creasap N, et al. Pten in stromal fibroblasts suppresses mammary epithelial tumours. Nature. 2009; 461:1084–91. [PubMed: 19847259]
28. Zabuawala T, Taffany DA, Sharma SM, Merchant A, Adair B, Srinivasan R, et al. An ets2-driven transcriptional program in tumor-associated macrophages promotes tumor metastasis. Cancer Res. 2010; 70:1323–33. [PubMed: 20145133]
29. Raghuwanshi SK, Nasser MW, Chen X, Strieter RM, Richardson RM. Depletion of {beta}-Arrestin-2 Promotes Tumor Growth and Angiogenesis in a Murine Model of Lung Cancer. J Immunol. 2008; 180:5699–706. [PubMed: 18390755]
30. Livak KJ, Schmittgen TD. Analysis of relative gene expression data using real-time quantitative PCR and the 2(-Delta Delta C(T)) Method. Methods. 2001; 25:402–8. [PubMed: 11846609]
31. Wolf R, Voscopoulos C, Winston J, Dharamsi A, Goldsmith P, Gunsior M, et al. Highly homologous hS100A15 and hS100A7 proteins are distinctly expressed in normal breast tissue and breast cancer. Cancer Lett. 2009; 277:101–7. [PubMed: 19136201]
32. Al-Bazz YO, Brown BL, Underwood JC, Stewart RL, Dobson PR. Immuno-analysis of phospho-Akt in primary human breast cancers. Int J Oncol. 2009; 35:1159–67. [PubMed: 19787271]
33. Dechow TN, Pedranzini L, Leitch A, Leslie K, Gerald WL, Linkov I, et al. Requirement of matrix metalloproteinase-9 for the transformation of human mammary epithelial cells by Stat3-C. Proc Natl Acad Sci U S A. 2004; 101:10602–7. [PubMed: 15249664]
34. Wiseman BS, Werb Z. Stromal effects on mammary gland development and breast cancer. Science. 2002; 296:1046–9. [PubMed: 12004111]
35. Kang JC, Chen JS, Lee CH, Chang JJ, Shieh YS. Intratumoral macrophage counts correlate with tumor progression in colorectal cancer. J Surg Oncol. 2010; 102:242–8. [PubMed: 20740582]
36. Stein M, Keshav S, Harris N, Gordon S. Interleukin 4 potently enhances murine macrophage mannose receptor activity: a marker of alternative immunologic macrophage activation. J Exp Med. 1992; 176:287–92. [PubMed: 1613462]
37. Wolf R, Howard OM, Dong HF, Voscopoulos C, Boeshans K, Winston J, et al. Chemotactic activity of S100A7 (Psoriasin) is mediated by the receptor for advanced glycation end products and potentiates inflammation with highly homologous but functionally distinct S100A15. J Immunol. 2008; 181:1499–506. [PubMed: 18606705]

38. Mantovani A, Schioppa T, Porta C, Allavena P, Sica A. Role of tumor-associated macrophages in tumor progression and invasion. Cancer Metastasis Rev. 2006; 25:315–22. [PubMed: 16967326]
39. Nicolini A, Carpi A, Rossi G. Cytokines in breast cancer. Cytokine Growth Factor Rev. 2006; 17:325–37. [PubMed: 16931107]
40. Weinstat-Saslow D, Merino MJ, Manrow RE, Lawrence JA, Bluth RF, Wittenbel KD, et al. Overexpression of cyclin D mRNA distinguishes invasive and in situ breast carcinomas from non-malignant lesions. Nat Med. 1995; 1:1257–60. [PubMed: 7489405]
41. Condeelis J, Pollard JW. Macrophages: obligate partners for tumor cell migration, invasion, and metastasis. Cell. 2006; 124:263–6. [PubMed: 16439202]
42. Riehl A, Nemeth J, Angel P, Hess J. The receptor RAGE: Bridging inflammation and cancer. Cell Commun Signal. 2009; 7:12. [PubMed: 19426472]
43. Taguchi A, Blood DC, del Toro G, Canet A, Lee DC, Qu W, et al. Blockade of RAGE- amphoterin signalling suppresses tumour growth and metastases. Nature. 2000; 405:354–60. [PubMed: 10830965]
44. Qian BZ, Li J, Zhang H, Kitamura T, Zhang J, Campion LR, et al. CCL2 recruits inflammatory monocytes to facilitate breast-tumour metastasis. Nature. 2011; 475:222–5. [PubMed: 21654748]
45. Saji H, Koike M, Yamori T, Saji S, Seiki M, Matsushima K, et al. Significant correlation of monocyte chemoattractant protein-1 expression with neovascularization and progression of breast carcinoma. Cancer. 2001; 92:1085–91. [PubMed: 11571719]
46. Ueno T, Toi M, Saji H, Muta M, Bando H, Kuroi K, et al. Significance of macrophage chemoattractant protein-1 in macrophage recruitment, angiogenesis, and survival in human breast cancer. Clin Cancer Res. 2000; 6:3282–9. [PubMed: 10955814]
47. Valkovic T, Lucin K, Krstulja M, Dobi-Babic R, Jonjic N. Expression of monocyte chemotactic protein-1 in human invasive ductal breast cancer. Pathol Res Pract. 1998; 194:335–40. [PubMed: 9651946]
48. McLean MH, Murray GI, Stewart KN, Norrie G, Mayer C, Hold GL, et al. The inflammatory microenvironment in colorectal neoplasia. PLoS One. 2011; 6:e15366. [PubMed: 21249124]
49. Nam JS, Kang MJ, Suchar AM, Shimamura T, Kohn EA, Michalowska AM, et al. Chemokine (C-C motif) ligand 2 mediates the prometastatic effect of dysadherin in human breast cancer cells. Cancer Res. 2006; 66:7176–84. [PubMed: 16849564]
50. Wang D, Wang H, Brown J, Daikoku T, Ning W, Shi Q, et al. CXCL1 induced by prostaglandin E2 promotes angiogenesis in colorectal cancer. J Exp Med. 2006; 203:941–51. [PubMed: 16567391]

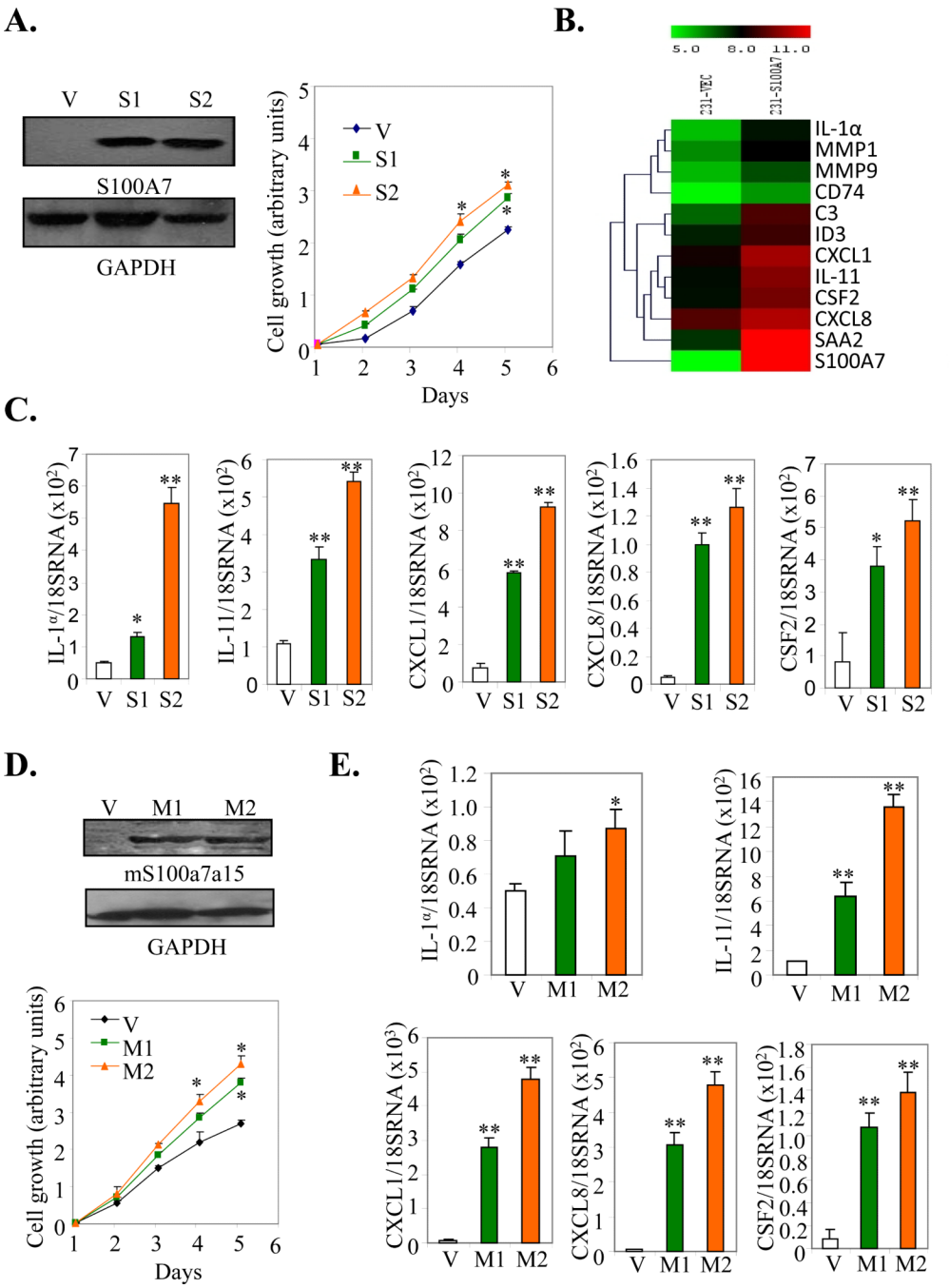

Figure 1. Effect of hS100A7 and mS100a7a15 overexpression on proliferation and pro-inflammatory gene expression

(A, *left*) The expression of hS100A7 in two different clones of MDA-MB-231 cells (S1 and S2) was analyzed by WB using hS100A7 specific antibody. GAPDH was used as the loading control. (A, *right*) Proliferation of hS100A7 expressing MDA-MB-231 (S1 and S2) and vector control cells (V) was analyzed using MTT assay. (B) Heat-map of differentially expressed genes in MDA-MB-231overexpressing hS100A7 (231-S100A7) compared to control (231-Vec). (C) Expression of transcripts for indicated inflammatory markers relative to GAPDH in Vec or hS100A7 overexpressing cells (S1 and S2) by q-PCR. (D, *upper*) The expression of mS100a7a15 in two different clones of MDA-MB-231 cells (M1 and M2) was

analyzed by WB using mS100a7a15 antibody. (D, *lower*) Proliferation of mS100a7a15 expressing MDA-MB-231 (M1 and M2) and Vec cells was analyzed using the MTT assay. (E) Expression of transcripts of inflammatory markers as analyzed by q-PCR in mS100a7a15 overexpressing clones M1 and M2. All the experiments were repeated three times and representative ones are shown. Graphs represent the mean ± SD for each experimental group.*, $p<0.05$ and **, $p<0.01$.

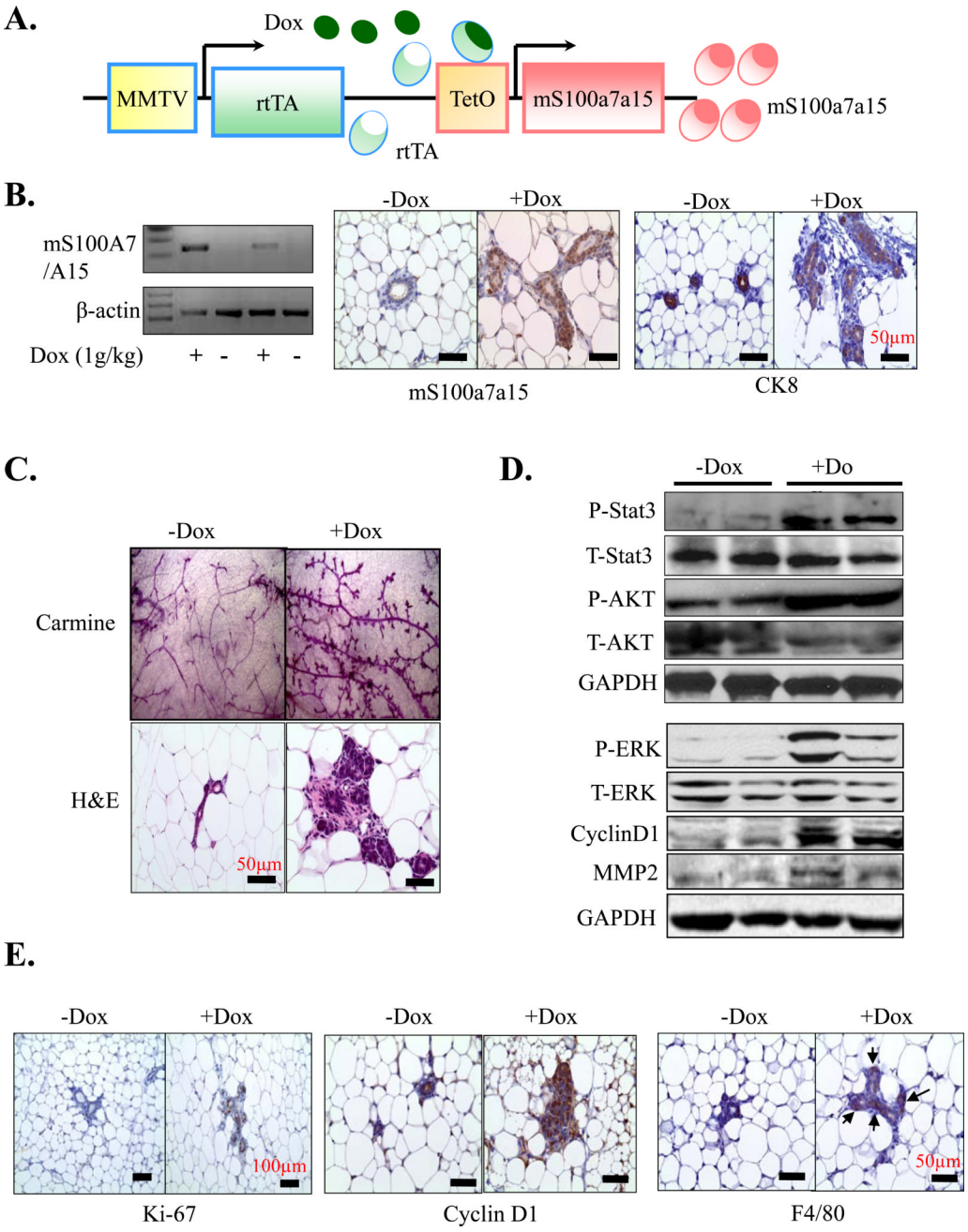

Figure 2. Characterization of the inducible, mammary-specific mS100a7a15 transgenic mouse model

(A) Schematic representation of the inducible, MMTV-mS100a7a15 (Tet-O, tet operator) mouse model system. (B, *left*) RT-PCR analysis of mS100a7a15 expression in MG of Dox induced and uninduced mice (n=5). (B, *right*) IHC analysis of mS100a7a15 and CK8 of MG from Dox treated (+Dox) and untreated (-Dox) mice. (C, *upper*) MG from Dox treated (+Dox) and untreated (-Dox) mice were subjected to whole-mount carmine staining (Original magnification of 40x) or (C, *lower*) H&E staining. (D) MG lysates (50 μg) from MMTV-mS100a7a15 mice treated with +Dox or -Dox were subjected to WB using phospho-STAT3, phospho-ERK, phospho-AKT (P-STAT3, P-ERK, P-AKT), cyclinD1 and MMP-2 antibodies. Blot showing anti-GAPDH indicates equal loading of lysates. (E) MG

isolated from +Dox and – Dox (n=5) treated mice were subjected to IHC of Ki-67, cyclin D1 and F4/80. Representative photomicrographs of five mammary tissues per experimental group.

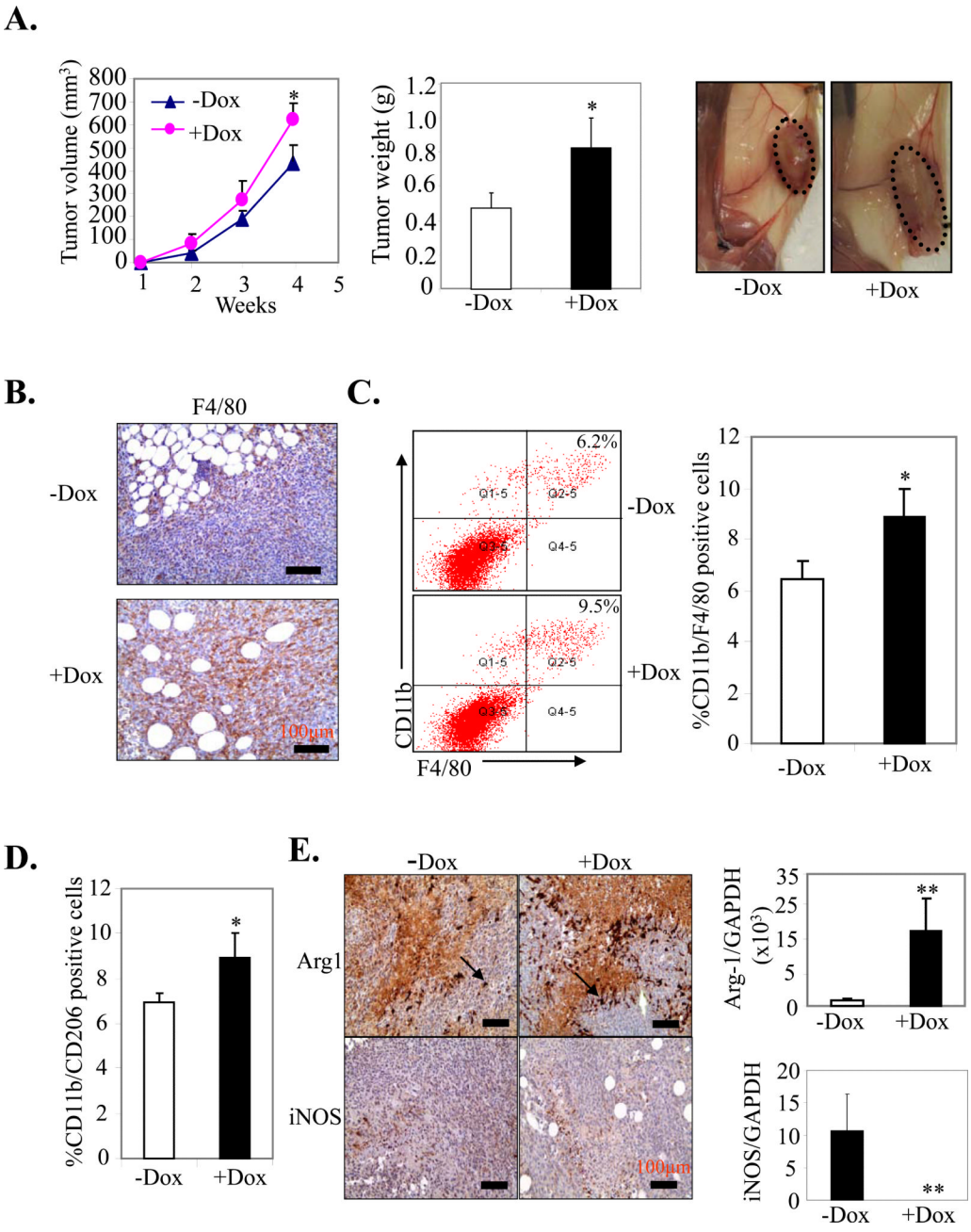

Figure 3. Effect of mS100a7a15 on tumor growth in orthotopic syngeneic model

(A, *left*) MVT-1 cells were injected into the MG of the MMTV-mS100a7a15 mice (n=5) and tumor volume was measured every week. (A, *middle*) After 28 days, the tumors were excised from mice and weighed. (A, *right*) Representative photograph of mice showing tumors dissected from different experimental groups. (B) MVT-1 cell line derived tumors from +Dox and –Dox MMTV-mS100a7a15 mice were subjected to IHC staining for macrophage marker, F4/80. (C) $CD11b^{+}F4/80^{+}$ cells and (D) $CD11b^{+}CD206^{+}$ were quantified by flow cytometry in disaggregated MVT1 primary tumors harvested 28 d after implantation from +Dox and – MMTV-mS100a7a15 mice. (E, *right*) IHC of Arginase-1 (Arg-1) and iNOS. (E, *left*) Expression of Arg-1 and iNOS by q-PCR. Data represent the mean ± SD of three independent experiments. *, $p<0.05$ and **, $p<0.01$.

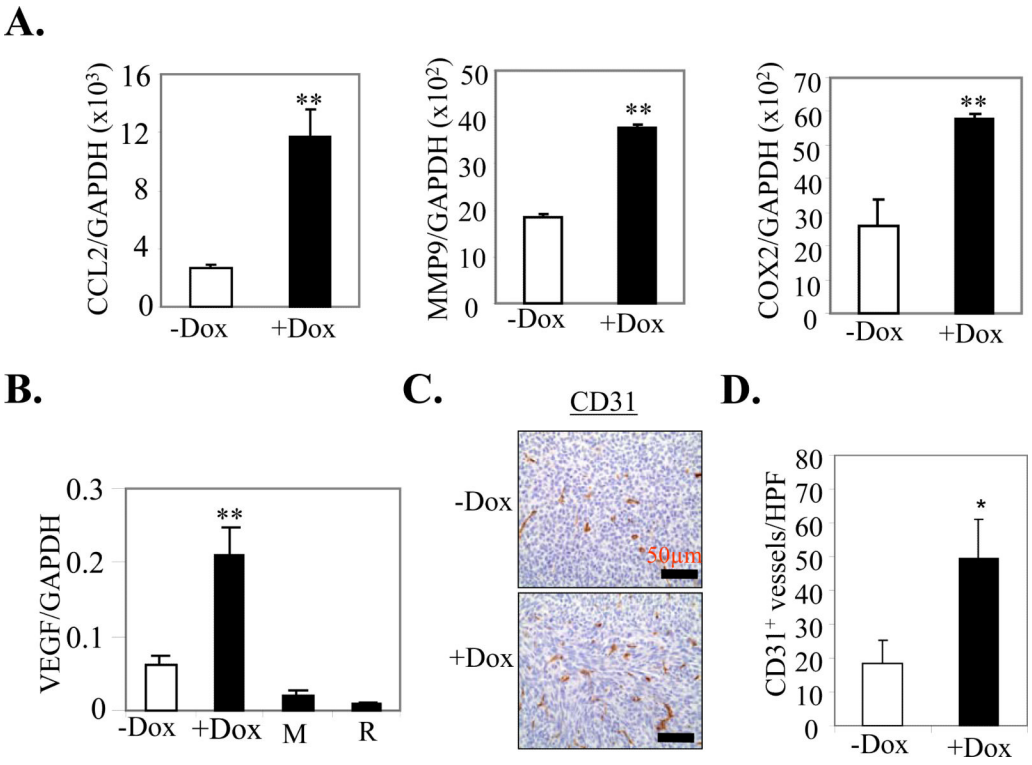

Figure 4. Effect of mS100a7a15 expression on pro-metastatic and angiogenic markers

(A) Gene expression was quantified by q-PCR in mammary tumors from +Dox and –Dox MMTV-mS100a7a15 mice (n=5). (B) VEGF expression in +Dox and –Dox MMTV-mS100a7a15 mice and MVT-1 (M) or RAW264.7 (R) cell lines. (C) Representative IHC with endothelial marker CD31 antibody to assess the number of blood vessels in tumors from Dox treated compared to untreated mice. (D) Bars represent the mean ± SD of the number of $CD31^+$ blood vessels shown in C counted in five random high power fields (HPF, 20X) per tissue section (n=5). *, $p<0.05$ and **, $p<0.01$.

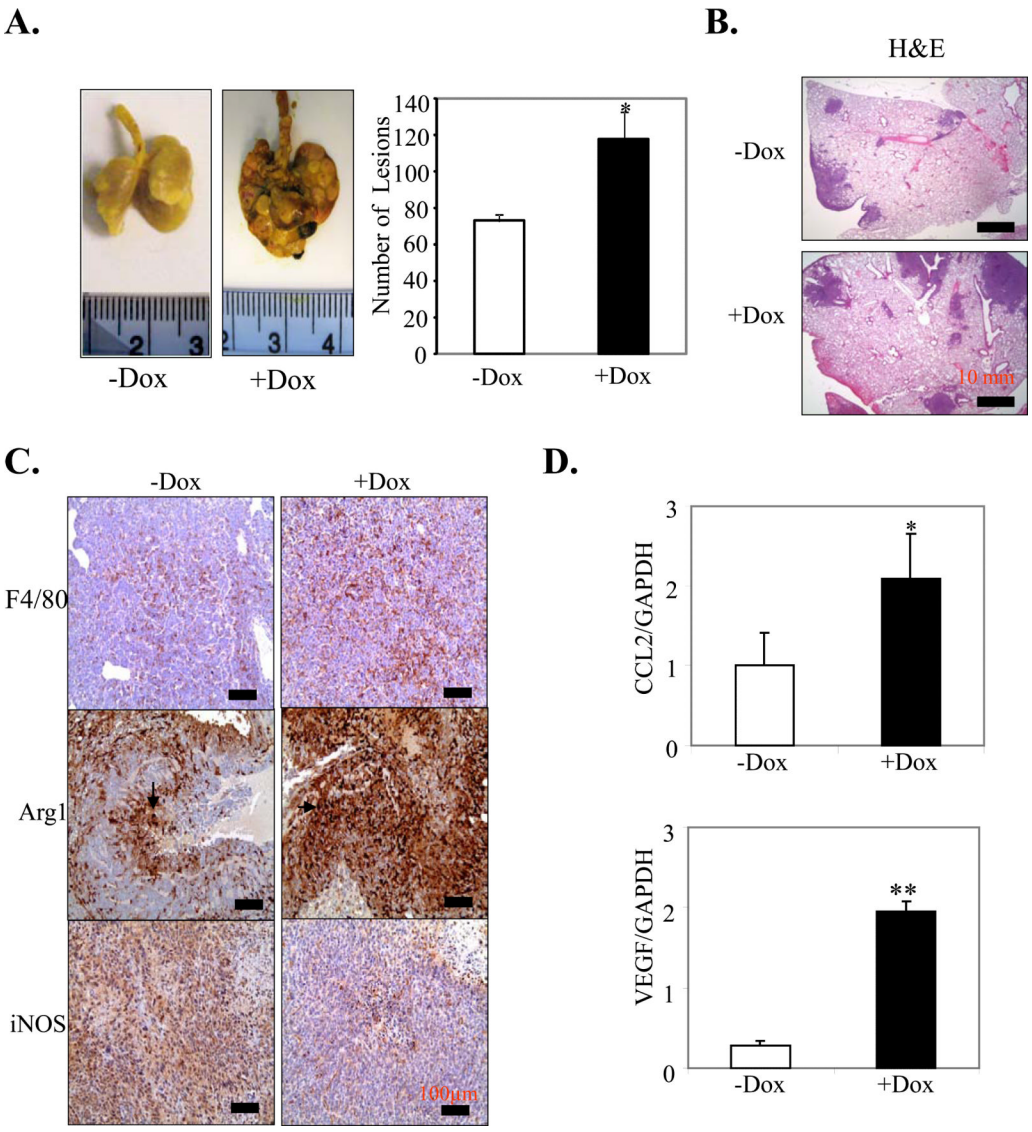

Figure 5. Effect of mS100a7a15 on metastasis and TAM infiltrations

MVT-1 cells were injected into the MG of the inducible MMTV-mS100a7a15 mice. (A, *left*), Representative photographs of metastatic nodules in the lung of +Dox (n=4) and –Dox (n=5) mice. (A, *right*), Lungs were removed and inflated with Bouin's fixative and number of metastatic nodules on the lungs was counted with the aid of a dissecting microscope (29). (B), H&E staining of metastatic nodules in the lung of Dox-treated MMTV-mS100a7a15 or untreated mice. (C), IHC of F4/80, Arg-1 and iNOS in metastatic lung tissues obtained from +Dox and –Dox MMTV-mS100a7a15 mice. (D) Expression of CCL2 and VEGF by q-PCR. Data represent the mean ± SD per experimental group. *, $p<0.05$ and **, $p<0.01$.

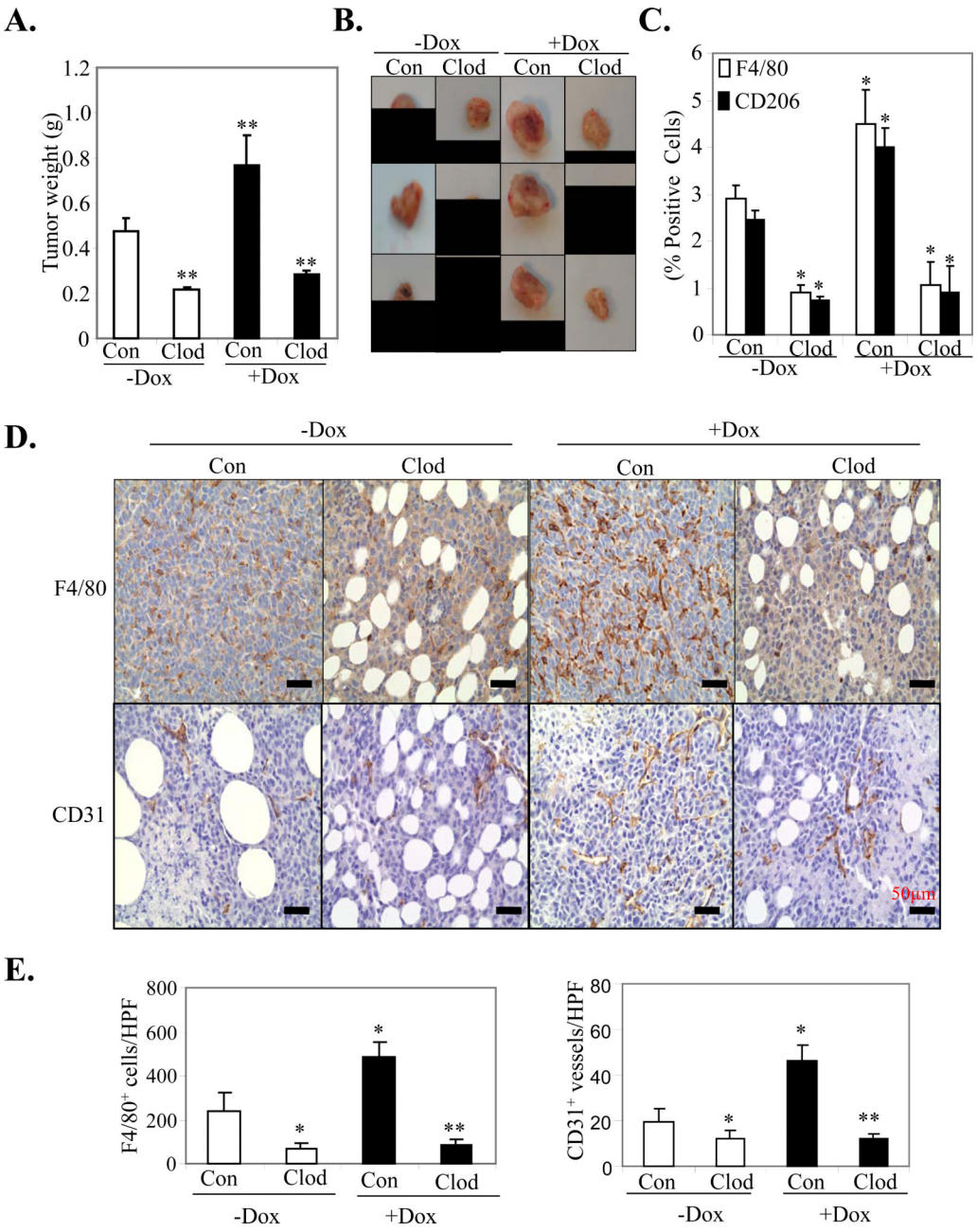

Figure 6. Effect of macrophage depletion on tumor growth and angiogenesis

(A) Growth of MVT-1 derived tumors in Dox- induced or uninduced MMTV-mS100a7a15 mice treated with either clodrolip or control-liposomes. (B) Representative photograph of tumors derived from different experimental groups. (C) Quantitative analyses of $F4/80^+$ macrophages (white columns) or $CD206^+$ M2 macrophages (black columns) by FACS. Graphs represent the mean ± SD (Control, $n = 4$; clodrolip, $n = 5$) *, $P < 0.05$; **, $P < 0.01$. (D) Representative IHC staining of mammary tumor sections treated with clodrolip and control-liposomes with macrophage marker F4/80 antibody (*upper*) and with endothelial marker CD31 antibody (*lower*) to assess the number of macrophages infiltrating into tumors and increase angiogenesis in tumors from Dox-treated compared to untreated mice. (E) Bars represent the mean ± SD of the number of $F4/80^+$ macrophages (*left*) and $CD31^+$ blood

vessels (*right*) as shown in D and counted in five random high power fields (HPF, 20X) per tissue section (Control, $n = 4$; clodrolip, $n = 5$) *, $P < 0.05$; **, $P < 0.01$.

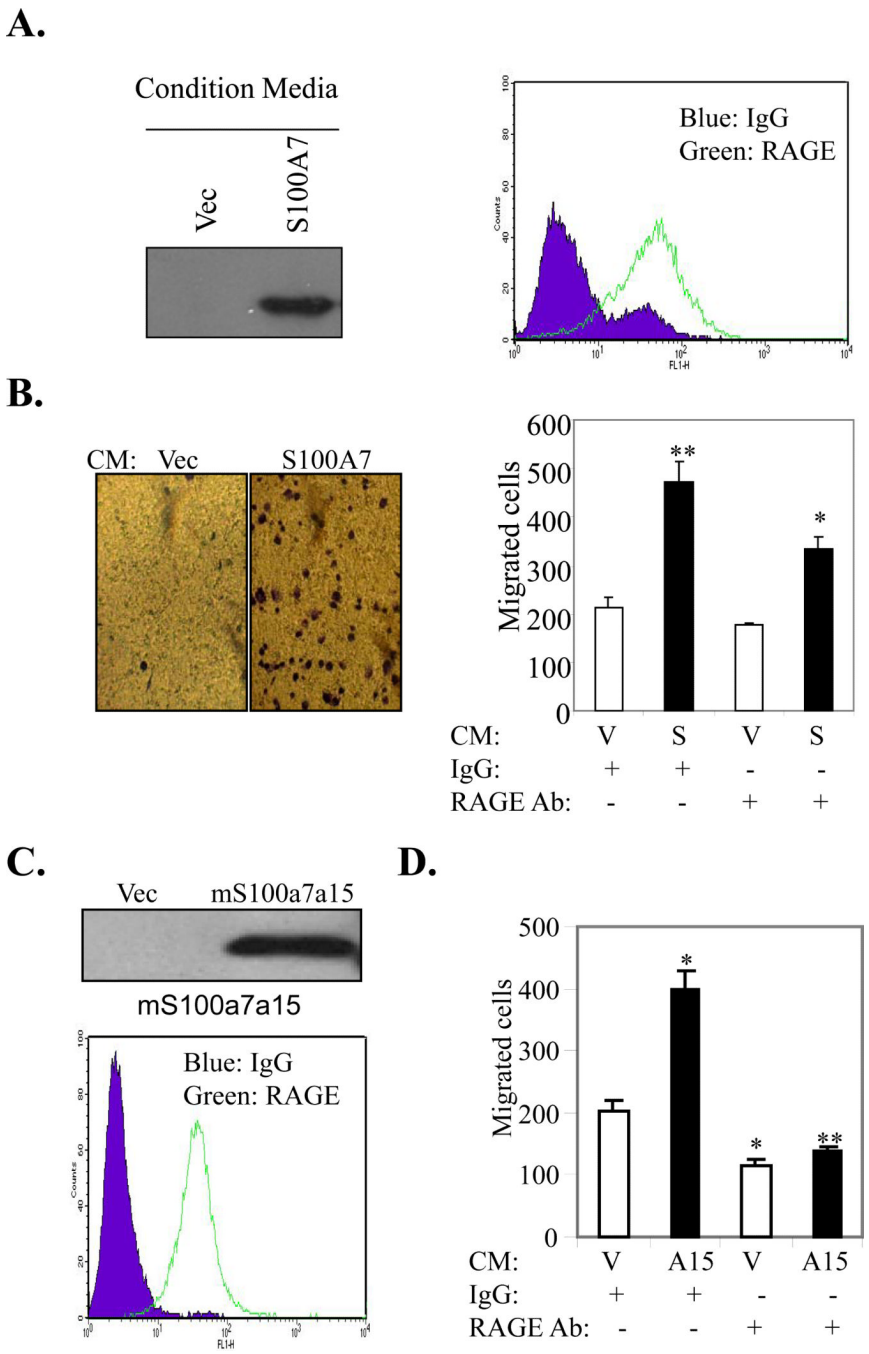

Figure 7. Role of RAGE in hS100A7 and mS100a7a15-induced chemotaxis of macrophages

(A) WB of CM obtained from Vec or hS100A7 overexpressing MDA-MB-231 cells. (A, *left*), FACS analysis of RAGE expression in TDM. (B, *left*) Representative photographs of migrated TDM under phase contrast microscope. (B, *right*) TDM were subjected to hS100A7 or Vec CM-induced migration in presence of RAGE neutralizing or control antibodies. (C, *upper*) WB of CM of Vec or mS100a7a15 overexpressing cells. (C, *lower*) FACS analysis of RAGE expression in MMR. (D) MMR were subjected to vector or mS100a7a15 CM-induced migration in presence of murine RAGE neutralizing or control antibodies. V represents vector, S represents hS100A7 and A15 represents mS100a7a15.

Graphs represent the mean ± SD for each experiment repeated three times with similar results.*, $p<0.05$ and **, $p<0.01$.